

RESEARCH

Open Access



Cholinergic signaling via the $\alpha 7$ nicotinic acetylcholine receptor regulates the migration of monocyte-derived macrophages during acute inflammation

Kasey R. Keever^{1,3}, Kui Cui¹, Jared L. Casteel^{1,3}, Sanjay Singh¹, Donald B. Hoover^{1,3}, David L. Williams^{2,3}, Valentin A. Pavlov^{4,5} and Valentin P. Yakubenko^{1,3*} 

Abstract

Background The involvement of the autonomic nervous system in the regulation of inflammation is an emerging concept with significant potential for clinical applications. Recent studies demonstrate that stimulating the vagus nerve activates the cholinergic anti-inflammatory pathway that inhibits pro-inflammatory cytokines and controls inflammation. The $\alpha 7$ nicotinic acetylcholine receptor ($\alpha 7$ nAChR) on macrophages plays a key role in mediating cholinergic anti-inflammatory effects through a downstream intracellular mechanism involving inhibition of NF- κ B signaling, which results in suppression of pro-inflammatory cytokine production. However, the role of the $\alpha 7$ nAChR in the regulation of other aspects of the immune response, including the recruitment of monocytes/macrophages to the site of inflammation remained poorly understood.

Results We observed an increased mortality in $\alpha 7$ nAChR-deficient mice (compared with wild-type controls) in mice with endotoxemia, which was paralleled with a significant reduction in the number of monocyte-derived macrophages in the lungs. Corroborating these results, fluorescently labeled $\alpha 7$ nAChR-deficient monocytes adoptively transferred to WT mice showed significantly diminished recruitment to the inflamed tissue. $\alpha 7$ nAChR deficiency did not affect monocyte 2D transmigration across an endothelial monolayer, but it significantly decreased the migration of macrophages in a 3D fibrin matrix. In vitro analysis of major adhesive receptors (L-selectin, $\beta 1$ and $\beta 2$ integrins) and chemokine receptors (CCR2 and CCR5) revealed reduced expression of integrin αM and αX on $\alpha 7$ nAChR-deficient macrophages. Decreased expression of $\alpha M\beta 2$ was confirmed on fluorescently labeled, adoptively transferred $\alpha 7$ nAChR-deficient macrophages in the lungs of endotoxemic mice, indicating a potential mechanism for $\alpha 7$ nAChR-mediated migration.

Conclusions We demonstrate a novel role for the $\alpha 7$ nAChR in mediating macrophage recruitment to inflamed tissue, which indicates an important new aspect of the cholinergic regulation of immune responses and inflammation.

Keywords Cholinergic anti-inflammatory pathway, $\alpha 7$ nAChR, Macrophage, Migration, Endotoxemia, Sepsis

*Correspondence:

Valentin P. Yakubenko
yakubenko@etsu.edu

Full list of author information is available at the end of the article



© The Author(s) 2023. **Open Access** This article is licensed under a Creative Commons Attribution 4.0 International License, which permits use, sharing, adaptation, distribution and reproduction in any medium or format, as long as you give appropriate credit to the original author(s) and the source, provide a link to the Creative Commons licence, and indicate if changes were made. The images or other third party material in this article are included in the article's Creative Commons licence, unless indicated otherwise in a credit line to the material. If material is not included in the article's Creative Commons licence and your intended use is not permitted by statutory regulation or exceeds the permitted use, you will need to obtain permission directly from the copyright holder. To view a copy of this licence, visit <http://creativecommons.org/licenses/by/4.0/>. The Creative Commons Public Domain Dedication waiver (<http://creativecommons.org/publicdomain/zero/1.0/>) applies to the data made available in this article, unless otherwise stated in a credit line to the data.

Background

Active research during the last 20 years has revealed the important role of the vagus nerve in the regulation of immunity and inflammation in a physiological mechanism termed *the inflammatory reflex* [1, 2]. In the inflammatory reflex, sensory (afferent) vagus nerve signaling is activated by cytokines and other inflammatory molecules in response to pathogens, injury, or other pathophysiological events [1, 3]. This signaling is integrated in the brainstem with motor (efferent) vagus nerve cholinergic signaling, which controls pro-inflammatory cytokine levels and inflammation [2, 4]. This efferent arm of the inflammatory reflex was termed *the cholinergic anti-inflammatory pathway* [2, 5]. The $\alpha 7$ nicotinic acetylcholine receptor ($\alpha 7$ nAChR) expressed on macrophages and other immune cells has been identified as a key mediator of cholinergic anti-inflammatory signaling [6, 7]. Stimulation of the $\alpha 7$ nAChR on macrophages activates downstream intracellular mechanisms, including suppression of NF- κ B activation and results in decreased production of TNF and other pro-inflammatory cytokines [8–11]. These discoveries opened an avenue of preclinical research revealing the anti-inflammatory efficacy of vagus nerve stimulation (VNS) and $\alpha 7$ nAChR agonists in endotoxemia, sepsis and many other inflammatory conditions [12, 13]. This research paved the way to recent successful clinical trials with VNS in patients with inflammatory disorders [14].

Murine endotoxemia and cecal ligation and puncture (CLP) have been widely used in studying the role of the $\alpha 7$ nAChR in the cholinergic regulation of inflammation. Endotoxemia, associated with robust systemic cytokine release and inflammation is considered by some as a model of gram negative sepsis, while CLP is a clinically relevant model of polymicrobial sepsis [15]. Sepsis is a life-threatening condition characterized by organ dysfunction resulting from an excessive inflammatory response to infection. This organ system dysfunction is correlated with higher long term mortality, even if patients recover from their illness in the hospital [16]. In mice, VNS or pharmacological cholinergic $\alpha 7$ nAChR activation suppresses pro-inflammatory cytokine levels and mitigate mortality in mice with endotoxemia and CLP [13, 17–20]. The role of macrophages in endotoxemia and sepsis is complex; some reports characterize macrophages as protective due to their crucial role in efferocytosis of neutrophils, phagocytosis of bacteria, and tissue repair, while other reports indicate their detrimental effects [21–23]. The role of $\alpha 7$ nAChR on macrophages in mediating cholinergic suppression of pro-inflammatory cytokine production in the cholinergic anti-inflammatory pathway has been characterized as a major mechanism underlying the neural control of immune

responses. However, other potential mechanisms, such as modulating the recruitment of monocytes/macrophages to damaged tissue, remain unclear.

In this study, we investigated the broader role of the $\alpha 7$ nAChR in inflammation by examining the migration and accumulation of macrophages during endotoxemia. We showed that the protective role of $\alpha 7$ nAChR in endotoxemia is positively correlated with monocyte/macrophage migration to the inflamed tissues. Moreover, we found that $\alpha 7$ nAChR-mediated migratory properties depend on the expression of a major adhesive receptor integrin $\alpha M\beta 2$ (CD11b/CD18), thus indicating an important molecular link between cholinergic signaling and macrophage motility. Therefore, these results reveal a novel protective mechanism of the cholinergic anti-inflammatory pathway.

Materials and methods

Reagents and antibodies

Reagents were purchased from Sigma-Aldrich (St. Louis, MO, USA), BioRad (Hercules, CA, USA), BioLegend (San Diego, CA, USA), and Thermo Fisher Scientific (Waltham, MA, USA). Lipopolysaccharide (LPS, endotoxin) derived from *E. coli* O55:B5, and PNU-282987 were purchased through Sigma-Aldrich. Antibodies against cell surface markers Ly6-G (clone 1A8), Ly6-C (clone HK1.4), αM (clone M1/70), αL (clone M17/4), F4/80 (clone BM8), αX (clone N418), and $\alpha 4$ (clone R1–2) are from eBioscience. Antibodies against Siglec F (clone 1RNM44N) and L-selectin (clone MEL-14) are from Invitrogen. Antibodies against CCR2 (clone SA203G11) and CCR5 (clone HM-CCR5) are from BioLegend.

Animals

Wild-type (WT; C57BL/6), stock #000664) and $\alpha 7$ nAChR-deficient ($\alpha 7$ nAChR^{-/-}; B6.129S7-Chrna7^{tm1Bay}/J, stock #003232) mouse colonies were purchased from Jackson Laboratory (Bar Harbor, ME, USA). The $\alpha 7$ nAChR deficient strain was backcrossed to C57BL/6 for eight generations. Mice aged between 8 and 12 weeks were used for the study. Similar age WT and $\alpha 7$ nAChR^{-/-} mice were employed for each experiment. No comparative analysis was conducted across mice of varying sexes and ages. All animal procedures were performed according to animal protocols approved by East Tennessee State University IACUC. Protocol number is P210903.

Endotoxemia

In survival experiments, male or female WT and $\alpha 7$ nAChR^{-/-} mice were intraperitoneally injected with a sublethal dose of LPS calculated based on body weight. Since LPS activity is slightly variable from bath to bath,

we evaluated the sublethal dose for each vial preparation using increasing doses of LPS (*E. coli* O55:B5) in C57BL/6J wild-type mice. Female mice are more resistant to LPS treatment compared to male mice [24, 25]. Therefore, a gender-specific dosing was applied to reach a similar percentage of lethality for male and female mice. Depending on the LPS bath preparation we used 7–8 mg/kg for males and 9–12 mg/kg for females. Notably, the same concentration of LPS was used for all groups in each experiment.

In all endotoxemia experiments, body temperature was monitored twice daily using a rectal probe connected to a ThermoWorks (American Fork, UT, USA) MicroTherma meter.

To examine macrophage accumulation in the lungs, male or female WT and $\alpha 7nAChR^{-/-}$ mice were given an intraperitoneal injection of LPS as described above. After 48h, mice were euthanized using Isothesia (Henry Schein Animal Health, Dublin, OH) and perfused, and lungs were removed. Lungs were digested using collagenase II as described below ("Flow Cytometry and Imaging Flow Cytometry Analyses" section) and prepared for flow cytometry. In an additional experiment, male and female WT mice were treated intraperitoneally with 3mg/kg PNU-282987, 15 min before the injection of LPS, to examine the effect of $\alpha 7nAChR$ stimulation on macrophage accumulation. Control mice received DMSO (vehicle) 15 min before LPS. Samples were incubated with anti- $\alpha M/PE-Cy7$, anti-CCR2/APC, anti-CCR5/PE-Cy7, anti-Siglec F/FITC, anti-Ly6-G/PE, anti-F4/80/PE, anti-F4/80/APC, and anti- $\alpha X/APC$ across multiple samples.

Isolation of peritoneal macrophages

Thioglycollate-induced peritoneal macrophages are a well-established source to study macrophage function in inflammatory conditions. Peritoneal macrophages from 8- to 12-week-old WT and $\alpha 7nAChR^{-/-}$ mice were collected via peritoneal lavage with 5mL of sterile PBS 72 h after intraperitoneal injection of 1mL 4% thioglycollate. Mice were euthanized via CO₂ asphyxiation before the collection procedure. The cells were counted and plated in petri dishes for 2 h in RPMI 1640 (Corning, Corning, NY) with 10% FBS and 1% penicillin/streptomycin, after which non-adherent cells were removed.

Isolation of monocytes from mouse bone marrow

The isolation of bone-marrow-derived monocytes provides a pure population of monocytes that exceed the number of monocytes obtained from the peripheral blood of mice by approximately 10 folds. Monocytes were isolated from the femoral and tibial bone marrow of WT and $\alpha 7nAChR^{-/-}$ mice by first flushing out bone

marrow with RPMI 1640, followed by lysis of red blood cells. Magnetic-assisted cell sorting (MACS) was then used to purify monocytes via a negative separation kit, following the manufacturer's protocol (Miltenyi Biotec, Gaithersburg, MD, USA). Purity of the isolated monocytes was analyzed by flow cytometry using antibodies to $\alpha M/PE-Cy7$, Ly6-G/PE, and Ly6-C/FITC. In all experiments, the purity was between 87% and 92%.

Adoptive transfer of monocytes in the model of endotoxemia

Monocytes were isolated from the bone marrow of WT and $\alpha 7nAChR^{-/-}$ mice, as above, and labeled with red PKH26 (WT), or green PKH67 ($\alpha 7nAChR^{-/-}$) fluorescent dyes. A total of 1×10^6 red and 1×10^6 green monocytes were mixed equally and injected into the tail veins of WT mice or $\alpha 7nAChR^{-/-}$ mice. These mice received a sub-lethal dose of LPS intraperitoneally within 5 min after injection of cells. After 48 h, the mice were sacrificed using Isothesia and perfused with PBS. Lungs, liver, and spleen were isolated and digested with 2mg/mL collagenase II (Sigma Aldrich, St Louis, MO, USA) prepared in HBSS as previously described [26]. Digested cell suspension was filtered through a 70 μ m cell strainer and any remaining red blood cells were lysed. Cell filtrate was incubated with a viability dye and analyzed using flow cytometry (Fortessa X-20, Becton Dickinson, Franklin Lakes, NJ, USA) and imaging flow cytometry (ImageStream Mark II, Amnis, Seattle, WA, USA) for the detection of fluorescently labeled cells. The dye colors were used with only WT cells in a separate experiment to confirm that dye color does not influence the result.

Adoptive transfer rescue in the model of endotoxemia

WT or $\alpha 7nAChR^{-/-}$ monocytes were isolated from bone marrow as described above in "Isolation of Monocytes from Mouse Bone Marrow" section. Freshly isolated cells, either WT or $\alpha 7nAChR^{-/-}$, were injected into the tail veins of WT or $\alpha 7nAChR^{-/-}$ recipient mice. Cell injection was immediately followed by a sub-lethal dose of LPS. In all adoptive transfer rescue experiments, body temperature and morbidity were monitored twice daily. Mortality rate was analyzed using the Kaplan–Meier method.

Flow cytometry and imaging flow cytometry analyses

Flow cytometry analysis was used to assess cell surface markers listed in "Reagents and Antibodies" section as well as determine the number of PKH26 and PKH67 positive cells in the lungs, liver, and spleen during adoptive transfer. For the analysis of cell surface markers, harvested cells were first incubated with FcR-Blocking solution (eBioscience) for 15 min on ice. Next, samples

of 2×10^6 cells were incubated with appropriate antibody panels for 30 min on ice. Cells were then washed and analyzed using the Fortessa X-20 (Becton Dickinson).

To detect labeled macrophages in tissue, the lungs, liver, and spleen were digested using 2mg/mL collagenase II (Sigma-Aldrich, St Louis, MO, USA) as described above in "Adoptive Transfer of Monocytes in the Model of Endotoxemia" section. Cell suspension was next pre-cleaned via filtering through a 70µm cell strainer. Cells were incubated with live/dead viability dye for 30 min on ice (Thermo Fisher, Waltham, MA, USA). PKH26 and PKH67 labeled macrophages within the digested organs were analyzed with flow cytometry (Fortessa X-20) and imaging flow cytometry (Image Stream Mark II, Amnis). For analysis of αM on labeled macrophages, preparation was carried out as above.

Imaging flow cytometry analysis results were analyzed using IDEAS 6.2 software. The PKH26 and PKH67 labeled cells were captured on channels 2 and 3, respectively.

Macrophage 3D migration assay

WT and α7nAChR^{-/-} peritoneal macrophages were labeled with PKH26 red fluorescent dye or PKH67 green fluorescent dye. An equal number of WT and α7nAChR^{-/-} were mixed and plated on the membranes of 6.5mm transwell inserts with 8µm pores (Costar, Corning, NY) pre-coated with 4µg/mL fibrinogen for 3 h. A 3-D fibrin gel was made by mixing 0.75mg/mL fibrinogen containing 1% FBS and 1% penicillin/streptomycin with 0.5 U/mL thrombin, at a total volume of 100µL per transwell. MCP-1 (30nM) or RANTES (12.8nM) were added to 100µL of HBSS containing 1% FBS and 1% penicillin/streptomycin and added to the top of the gel to initiate migration. Transwells were incubated for 48h at 37 °C in 5% CO₂ in a 24-well plate. In each well, 650µL of HBSS containing 1% FBS and 1% penicillin/streptomycin was added beneath the transwell insert to prevent drying of the gel during incubation. Experiment run in two independent replicates with wells of each respective cytokine plated in triplicate. Migrating cells were detected using confocal microscopy (Leica TCS SP8), and results were analyzed with IMARIS 8.0 software. Wells showing migrated cells were used in statistical analysis, MCP-1 (n = 4) and RANTES (n = 3).

qRT-PCR

Prior to RNA isolation, peritoneal macrophages were incubated overnight with LPS (10ng/mL) and PNU-282897 (30µM). Total RNA was extracted from thioglycolate-induced mouse peritoneal macrophages using the PureLink RNA Mini Kit (Invitrogen, Carlsbad, CA, USA). Reverse transcription was performed using the

iScript cDNA Synthesis Kit (Bio Rad, Hercules, CA, USA). Roughly 0.8–1.0µg of cDNA was synthesized in a 20µL reaction volume, per the kit instructions. Real-time PCR reactions were set up in a 96-well qPCR plate using IQ SYBR Green Supermix (Biorad, Hercules, CA, USA) and run using the CFX96 Real Time Thermal Cycler fitted with a C1000 lid (BioRad). Each sample was plated in duplicate. Specific primers for each target were designed and are listed in Table 1 (Integrated DNA Technologies, Coralville, IA). Primer sequences were derived from previously published studies and verified using NCBI Blast and IDT Oligo Analyzer [27, 28]. Fold changes were normalized to GAPDH. Relative expression of each target was calculated using the Livak Method [29].

Trans-endothelial migration assay

Endothelial cells (HUVECS) were labeled using CellVue Claret (Sigma-Aldrich, St-Louis, MO) and incubated overnight on the membranes of 6.5mm transwell inserts with 8µm pores (Costar, Corning, NY) to form a monolayer. Non-adhered endothelial cells were gently washed out. WT and α7nAChR^{-/-} monocytes were isolated from bone marrow using magnetic-assisted cell sorting as described above in methods "Isolation of Monocytes from Mouse Bone Marrow" section. Isolated monocytes were labeled using either PKH67 (green) or PKH26 (red), with colors switched to confirm that dye color does not influence the result. Stained monocytes were added on top of the endothelial cells. MCP-1 (30nM) or RANTES (12.8nM) were added to the bottom chamber to start

Table 1. Primers sequence used for qPCR.

Primer	Sequence (5'-3')	References
αX forward	CTGGATAGCCTTCTTCTGCT	[30]
αX reverse	GCACACTGTGTCCGAAGCTCA	[30]
αM forward	TCCGGTAGCATCAACAACAT	[31]
αM reverse	GGTGAAGTGAATCCGGAAGT	[31]
αD forward	GGAACCGAATCAAGGTCAAGT	[32]
αD reverse	ATCCATTGAGAGAGCTGAGCTG	[32]
CCR2 forward	ACAGCTCAGGATTAACAGGGACTTG	[27]
CCR2 reverse	ACCACTTGCATGCACACATGAC	[27]
CCR5 forward	TCCGTTCCCTACAAGAGA	[28]
CCR5 reverse	TTGGCAGGGTGTGACATAC	[28]
MCP-1 forward	TGGAGCATCCACGTGTTGGC	[33]
MCP-1 reverse	ACTACAGCTTCTTTGGGACA	[33]
RANTES forward	GCTTCCCTGTGCTGCTTGGCTC	[34]
RANTES reverse	AGATGCCCATTTTCCAGGACC	[34]
β1 forward	GTGACCCATTGCAAGGAGAAGGA	[35]
β1 reverse	GTCATGAATTATCATTAAGTTTCCA	[35]
GAPDH forward	AAGGTCATCCCAGAGCTGAA	[36]
GAPDH reverse	CTGCTTACCACCTTCTTGA	[36]

migration, along with media containing 650 μ L of HBSS with 1% FBS and 2% penicillin/streptomycin to prevent drying. Each respective cytokine was plated in triplicate and the transmigration had three independent replicates. After 3 h, the migration was evaluated by confocal microscopy (Leica TCS SP8). Results were analyzed using IMARIS 8.0. Transwells with well-demarcated HUVEC monolayers were used for analysis, MCP-1 ($n=6$), and RANTES ($n=9$).

Isolation of peripheral blood monocytes

To evaluate the potential changes in adhesion receptor expressions on circulation monocytes after the LPS challenge, monocytes were isolated from the peripheral blood of WT and $\alpha 7nAChR^{-/-}$ mice. Male mice were injected with 8 μ g LPS per gram of body weight. After 3 h, mice were euthanized using Isothesia, and blood was collected in EDTA (200mM) coated syringes through cardiac puncture. Each mouse yielded 500–700 μ L of blood, which was diluted using an equal volume of balanced salt solution, prepared as instructed in the Cytiva Ficoll–Paque protocol. The monocytes were separated from whole blood using Ficoll–Paque 1.084 (Cytiva) according to manufacturer instructions. Isolated monocytes were then prepared for flow cytometry using anti-Ly6-C/FITC, anti- α M/PE-Cy7, anti- α L/APC, anti-L-selectin/PE, and anti- α 4/PE across multiple samples.

Statistical Analysis

Experimental data were analyzed using a two-tailed student's t test. Results are given as mean \pm SEM. Survival experiments were analyzed using the Kaplan Meier Method and Log Rank Test. Quantitative Real-Time PCR data were analyzed using the Livak Method. Values of $p < 0.05$ were considered to be statistically significant.

Results

7nAChR deficiency results in increased mortality and decreased macrophage accumulation in the lungs, while activation of $\alpha 7nAChR$ increases macrophage accumulation during endotoxemia

The anti-inflammatory effects of $\alpha 7nAChR$ activation using small molecule agonists have been extensively studied in mice with endotoxemia and CLP [9, 18, 19]. For instance, administering a partially selective $\alpha 7nAChR$ agonist, GTS-21, or choline—a product of acetylcholine degradation and a selective endogenous $\alpha 7nAChR$ agonist suppresses circulating pro-inflammatory cytokine levels, which is linked to reduced NF- κ B activation and increased survival in endotoxic mice and rats [11, 19]. However, the role of $\alpha 7nAChR$ deficiency on survival in endotoxemia and macrophage migration into tissues was not previously investigated.

We first evaluated the impact of $\alpha 7nAChR$ deficiency on morbidity during endotoxemia. Wild-type (WT) and $\alpha 7nAChR^{-/-}$ mice, both male and female ($n=10$ /strain), were injected with LPS and morbidity was monitored for 4 days. $\alpha 7nAChR$ deficiency significantly reduced the survival rates, exhibiting a similar pattern in both female ($p < 0.05$) and male ($p < 0.01$) mice (Fig. 1A, C). This reduction in survival correlated with a decrease in body temperature that indicated the severity of induced endotoxemia (Fig. 1B, D).

The recruitment of monocytes/macrophages into the lungs can have a protective outcome during endotoxemia [26, 37–39]. Therefore, we reasoned that decreased macrophage accumulation in lungs could be responsible for the increased mortality of $\alpha 7nAChR^{-/-}$ mice. To provide insight, age-matched WT and $\alpha 7nAChR^{-/-}$ mice were injected with LPS ($n=5$ /group) and the severity of endotoxemia was verified by a drop in body temperature after 48 h (Fig. 2B). After 48 h, the lungs were collected and digested to analyze leukocyte populations using flow cytometry (Fig. 2A). Live cells were selected using a viability dye, and specific markers were used to evaluate different leukocyte subsets. Neutrophils were analyzed as CD11b+, Ly6-G+, and F4/80-. Monocyte-derived macrophages were identified as CD11b+, F4/80+, and Ly6-G-, while alveolar macrophages were selected as F4/80+, CD11b-, and Siglec F+. The gating strategies for monocyte-derived and alveolar macrophages are depicted in Additional file 1: Figs. S1 and S2, respectively. We observed that the percentage of monocyte-derived macrophages in the lungs of $\alpha 7nAChR^{-/-}$ mice was significantly lower. The number of resident alveolar macrophages and neutrophils was not markedly different (Fig. 2B).

To assess the impact of $\alpha 7nAChR$ activation on macrophage accumulation, we treated WT mice with either LPS and DMSO (vehicle) or LPS with $\alpha 7nAChR$ agonist PNU-282987 ($n=7$ /group) (Fig. 2C). 3mg/kg PNU-282987 dissolved in DMSO or DMSO alone were administered 15 min prior to LPS injection as previously described [38]. Body temperature of mice receiving treatment with PNU-282987 was significantly higher at 48 h when compared to LPS only control. Using the same gating strategy for leukocyte subtypes, we observed that pre-treatment with PNU-282987 significantly increased the percentage of viable macrophages in the lungs and decreased the percentage of viable neutrophils (Fig. 2C, D). Interestingly, the proportion of viable resident alveolar macrophages in the lungs did not change with PNU-282987 treatment (Fig. 2D), but the absolute cell count was increased in PNU-282987-treated mice (Additional file 1: Fig. S2).

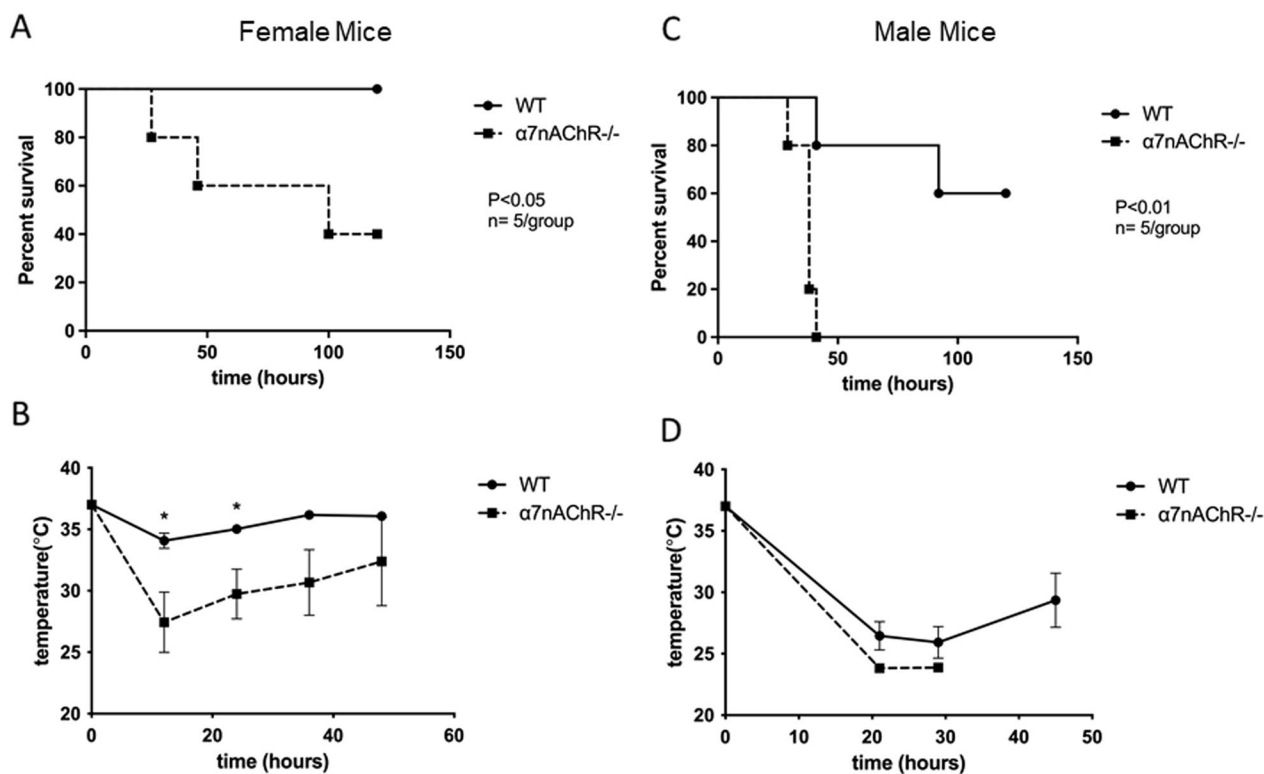


Fig. 1 HYPERLINK "sps:fig1||locator:gr1||MediaObject:0" $\alpha 7nAChR$ is protective during endotoxemia. **A** Survival curves after intraperitoneal administration of LPS to induce endotoxemia in female mice. (WT, $n = 5$; $\alpha 7nAChR^{-/-}$, $n = 5$). **B** After injection of LPS, a decrease in body temperature to 21–27 °C confirmed the development of endotoxemia. **C** Survival curves after LPS-induced endotoxemia in male mice. WT ($n = 5$) and $\alpha 7nAChR^{-/-}$ ($n = 5$). **D** Body temperature drop in male mice. Statistical significance of survival curves was assessed by the Kaplan–Meier method. Temperature data are shown as mean \pm SEM, * $P < 0.05$

Multiple mechanisms can contribute to the reduced accumulation of macrophages in the lungs during endotoxemia, including decreased monocyte/macrophage infiltration, increased apoptosis and promoted necrosis. Analysis with Annexin V staining did not reveal a significant difference in the amount of apoptotic or necrotic (late apoptotic) macrophages (Additional file 1: Fig. S3A–C). Notably, the number of necrotic neutrophils was also similar (Additional file 1: Fig. S3D). Together, these findings suggest that $\alpha 7nAChR$ -dependent macrophage accumulation is reliant on monocyte/macrophage migration.

$\alpha 7nAChR$ deficiency reduces the recruitment of monocyte-derived macrophages to the lungs during endotoxemia

To further assess the role of $\alpha 7nAChR$ in monocyte/macrophage migration, we conducted an in vivo adoptive transfer tracking experiment in the same model of endotoxemia to examine monocyte recruitment to the lungs, liver, and spleen. Fluorescently labeled WT and $\alpha 7nAChR^{-/-}$ monocytes were injected intravenously to recipient mice, as depicted in Fig. 3A. Monocytes were

isolated from bone marrow by negative selection (87–92% purity, Fig. 3B) and labeled with either green PKH67 ($\alpha 7nAChR^{-/-}$) or red PKH26 (WT) fluorescent dyes. WT and $\alpha 7nAChR^{-/-}$ monocytes were mixed in equal proportions and injected into recipient mice immediately followed by a sub-lethal dose of LPS. The cell mixture proportion was validated by fluorescent microscopy of a Cytospin slide (Additional file 1: Fig. S4A). After 48 h, the lungs, spleen and liver were digested for flow cytometry analysis to identify labeled, migrated macrophages (Fig. 3C). Flow cytometry data for the liver and spleen are shown in Additional file 1: Fig. S5. In addition, Imaging Flow Cytometry (Amnis) was employed to verify macrophage integrity, morphology and labeling (Fig. 3D). Our analysis revealed that lungs and other organs of WT recipient mice accumulate a significantly lower number of donor $\alpha 7nAChR^{-/-}$ macrophages compared to donor WT macrophages (Fig. 3E).

An overall similar trend was observed in the adoptive transfer of WT and $\alpha 7nAChR^{-/-}$ monocytes to $\alpha 7nAChR^{-/-}$ recipient mice (Fig. 4) that indicates that other cell types expressing $\alpha 7nAChR$ do not significantly

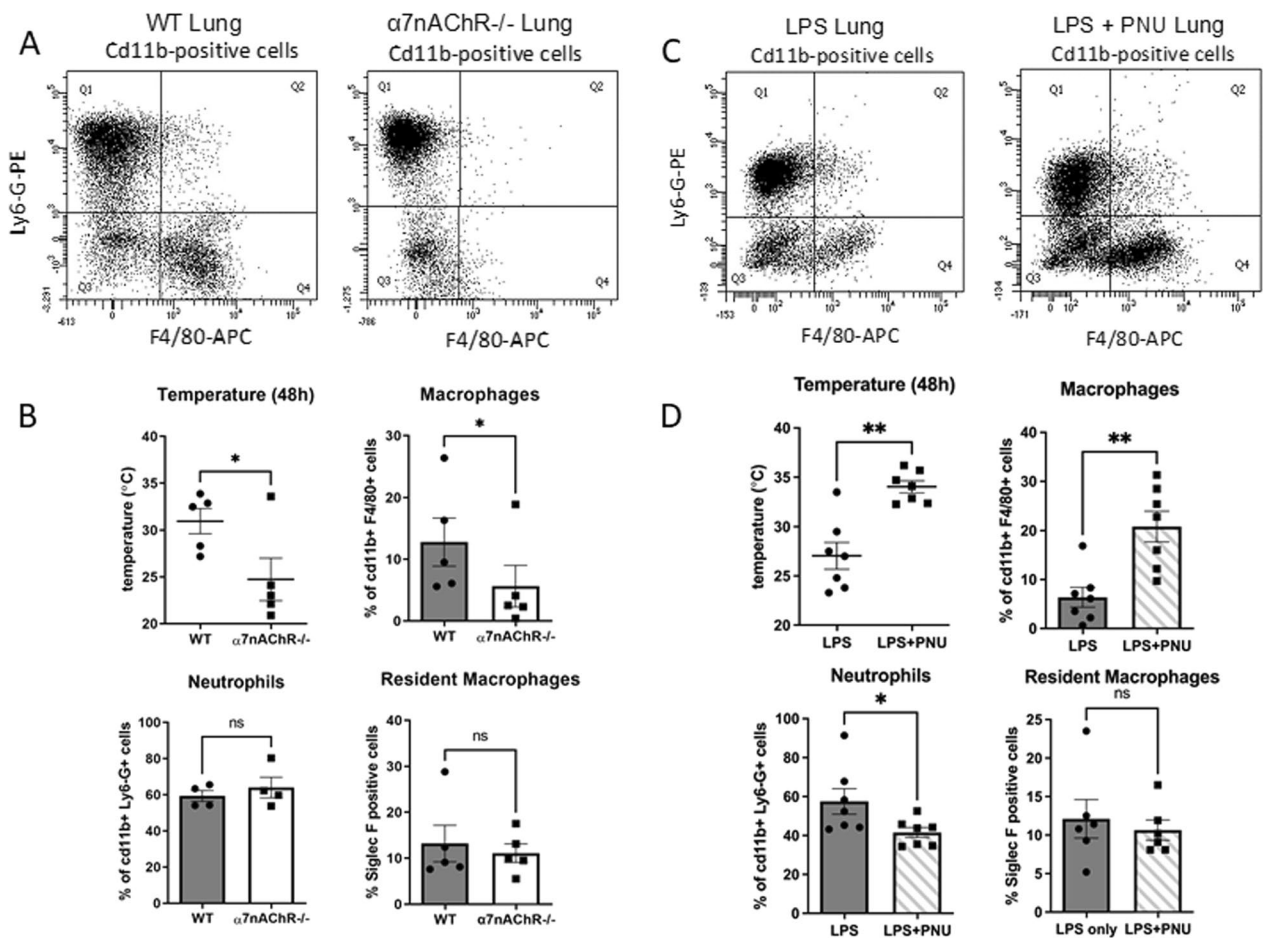


Fig. 2 Macrophage accumulation in the lungs is affected by $\alpha 7nAChR$ signaling. **A** WT and $\alpha 7nAChR^{-/-}$ mice were injected with a sublethal dose of LPS. After 48h lungs were removed, digested, and analyzed using flow cytometry. CD11b-positive cells were selected and tested with antibodies against Ly6-G and F4/80 to identify neutrophils and macrophages, respectively. Results were analyzed and calculated using FACSDiva software and GraphPad Prism. **B** Plots representing the number of WT and $\alpha 7nAChR^{-/-}$ macrophages (top right, $n = 5$ /group), neutrophils (bottom left, $n = 4$ /group), and resident macrophages (bottom right, $n = 5$ /group) in digested lungs. Residents were identified as CD11b-F4/80 + Siglec F +. Body temperature at 48h is shown at top right ($n = 7$ /group). **C** WT mice were injected with either a sublethal dose of LPS or 3mg/kg PNU-282987 followed by LPS 15 min later. The dose of LPS used was higher than for part A to generate more severe conditions for WT mice. After 48h lungs were removed, digested and analyzed using flow cytometry. CD11b positive cells and residents were selected and analyzed as above. Results were analyzed with FACSDiva software and calculated with GraphPad Prism. **D** Plots depicting the number of macrophages (top right, $n = 7$ /group), neutrophils (bottom left, $n = 7$ /group), and resident macrophages (bottom right, $n = 6$ /group). Body temperature at 48h is shown at top left ($n = 7$ /group). Statistical analysis was performed using a paired t test

influence the migration of monocytes/macrophages to tissue. Therefore, the expression of $\alpha 7nAChR$ on the monocyte/macrophage surface is critical for effective cell migration.

It is worth noting that PKH67 and PKH26 are widely used membrane stains and that we have previously demonstrated that switching red and green dye colors does not impact the results of our adoptive transfer experiments [32, 40, 41]. In an additional experiment, the adoptive transfer approach was performed using only WT monocytes labeled with PKH26 or PKH67 dyes, and no significant difference was observed in the number

of PKH26- or PKH-67-labeled WT macrophages in the inflamed tissue (Additional file 1: Fig. S4C,D).

Trans-endothelial migration of monocytes is not affected by $\alpha 7nAChR$ deficiency

Trans-endothelial migration is a critical step in the recruitment of monocytes from the blood into inflamed tissues. We tested whether $\alpha 7nAChR$ deficiency affects this process. A diagram depicting the experimental setup is shown in Additional file 1: Fig. S6A. After a 3-h incubation, cells that had crossed the endothelial cell monolayer were visualized using confocal microscopy, and images

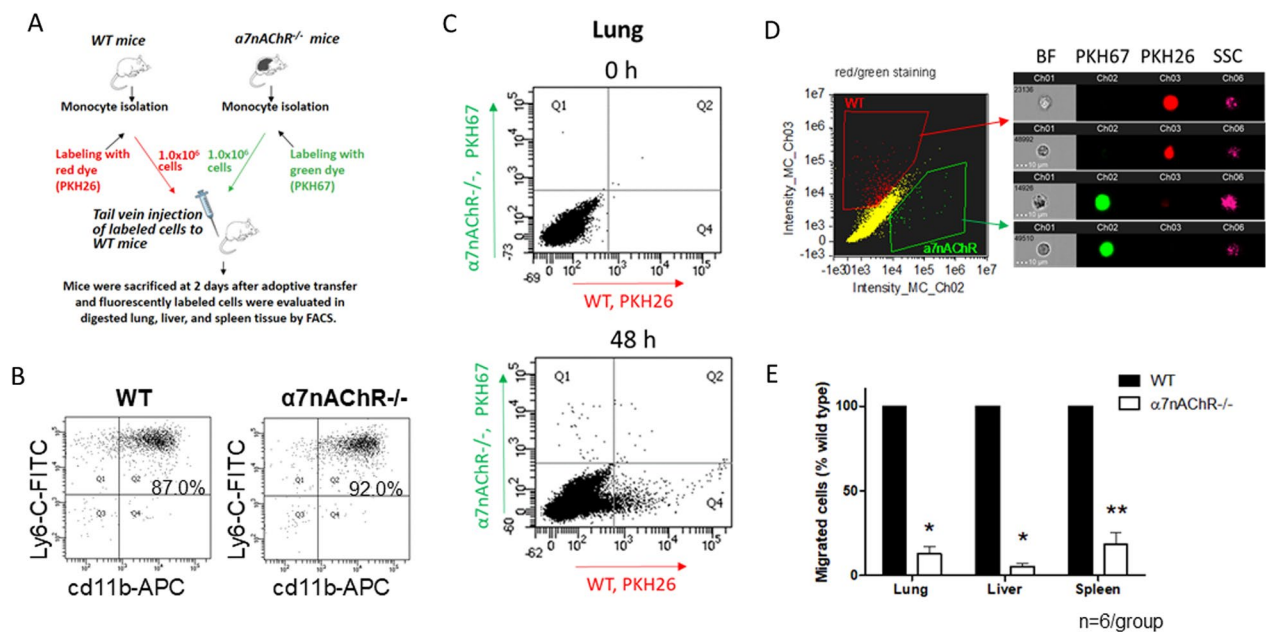


Fig. 3 $\alpha 7nAChR$ deficiency impedes the migration of macrophages to organs during LPS-induced endotoxemia. **A** Schematic representation of the experimental design. Monocytes were isolated from bone marrow of male WT and $\alpha 7nAChR^{-/-}$ mice via MACS. Cells were labeled with red (WT) or green ($\alpha 7nAChR^{-/-}$) fluorescent dyes, mixed in equal proportion and injected in tail vein of male WT recipient mice. After 48 h, the lung, liver and spleen were isolated, digested and analyzed using flow cytometry. **B** Representative dot plots of monocyte purity analysis. Isolated monocytes were labeled with anti-CD11b (APC) and anti-Ly6-G (FITC). Monocyte population is visible in Q2. **C** Representative results of flow cytometry analysis are shown. The leukocyte distribution in lungs before the adoptive transfer (Upper panel) and at 48 h after adoptive transfer and LPS administration (Lower panel) are presented. Data were analyzed using FACSDiva software. Migrated WT macrophages (red) were detected in Quadrant 4; $\alpha 7nAChR^{-/-}$ macrophages (green) were detected in Quadrant 1. **D** Imaging flow cytometry of labeled macrophages. (BF = bright field, SSC = side scattering). **E** Bar graphs representing the amount of WT and $\alpha 7nAChR$ -deficient macrophages detected in lungs, liver, and spleen by flow cytometry, ($n = 6$). Statistical analysis was performed using student's *t* test. * $P < 0.05$, ** $P < 0.01$

were reconstructed using IMARIS 8.0 software (Additional file 1: Fig. S6B). Notably, we observed no significant difference in the number of translocated WT and $\alpha 7nAChR^{-/-}$ monocytes in response to MCP-1 or RANTES (Additional file 1: Fig. S6C).

Because αM , αL , $\alpha 4$, and L-selectin are adhesion receptors and crucial in the trans-endothelial migration process, we examined their expression on the cell surface of mouse peripheral blood monocytes using flow cytometry. Monocytes were gated based on Ly6-C positivity before assessing the receptors relative expression in mean fluorescence intensity (MFI). We found no significant difference in MFI or the percentage of $\alpha L+$, L-selectin+, $\alpha 4+$, or $\alpha M+$ cells between WT and $\alpha 7nAChR^{-/-}$ mice (Additional file 1: Fig. S6D). These findings confirm that $\alpha 7nAChR$ deficiency does not impact the ability of isolated monocytes to migrate across an endothelial monolayer.

$\alpha 7nAChR$ deficiency reduces the migratory ability of macrophages in a 3D fibrin matrix along a chemokine gradient

To support our *in vivo* findings, we conducted an *in vitro* experiment to investigate the impact of

$\alpha 7nAChR$ on macrophage migration within a 3D matrix. WT and $\alpha 7nAChR^{-/-}$ macrophages were allowed to migrate through a 3D fibrin matrix within a transwell insert in response to a gradient of either MCP-1 or RANTES. A schematic diagram of the experimental setup is illustrated in Fig. 5A. Equal proportions (7.5×10^5) of fluorescently labeled WT (PKH26, red) and $\alpha 7nAChR^{-/-}$ (PKH67, green) macrophages were placed on the membrane of the insert before the addition of the matrix. MCP-1 (30nM) or RANTES (12.8nM) were then added to the top of the fibrin matrix to initiate migration. After 48 h of incubation at 37 °C and 5% CO₂, migrated cells were visualized using confocal microscopy (Fig. 5B, C) and images were reconstructed using IMARIS 8.0 software.

$\alpha 7nAChR^{-/-}$ macrophages exhibited significantly reduced migration in response to a RANTES gradient compared to WT macrophages (Fig. 5D). Although the response to an MCP-1 gradient showed a similar pattern, it did not reach statistical significance. These findings complement our *in vivo* results and support the suggestion that $\alpha 7nAChR$ deficiency may alter the expression of chemokine receptors and/or adhesive receptors.

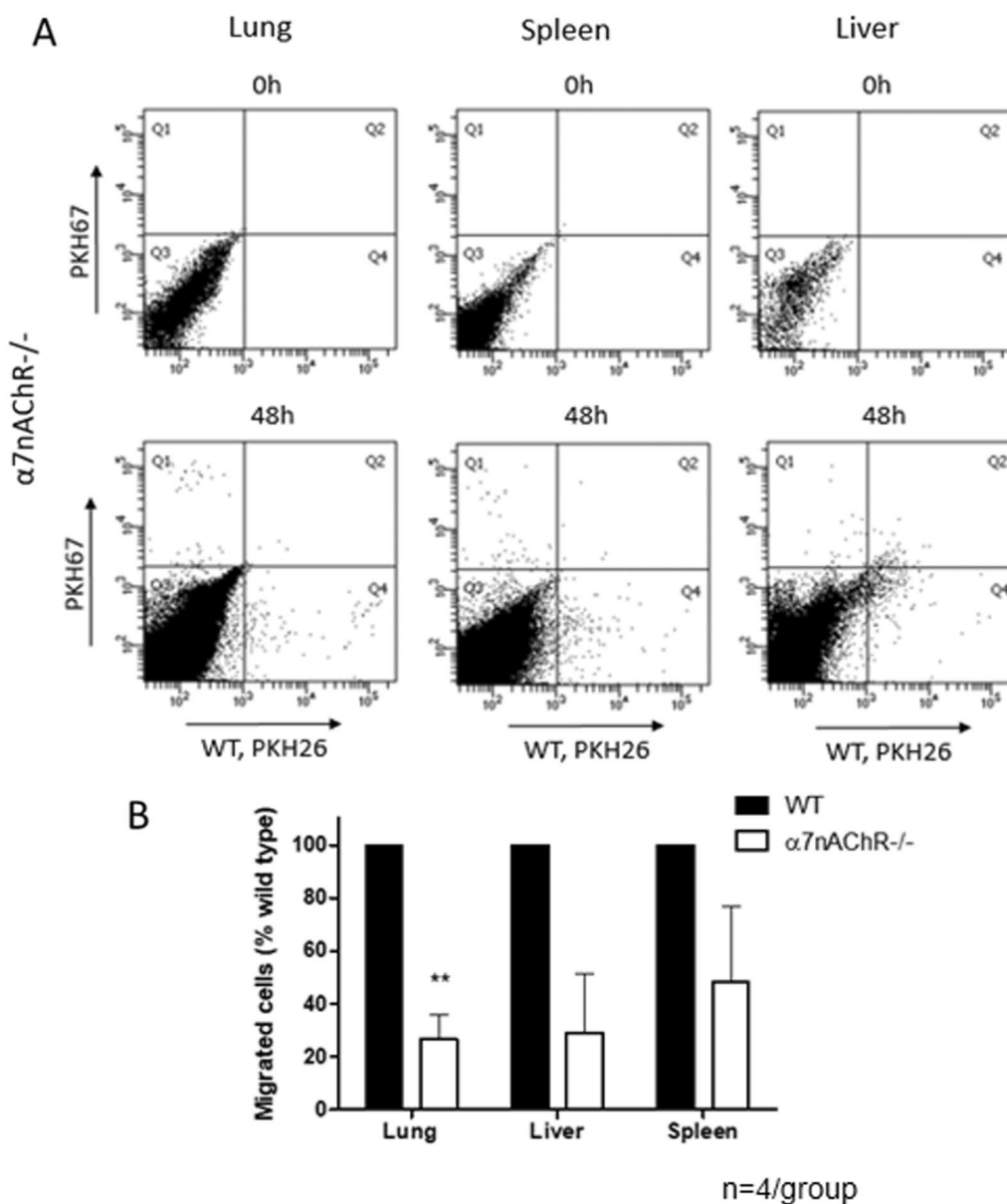


Fig. 4 Effect of $\alpha 7nAChR$ deficiency on migration does not depend on other cell types. **A** Representative dot plots of flow cytometry showing migrated red (WT) and green ($\alpha 7nAChR^{-/-}$) monocytes in male $\alpha 7nAChR^{-/-}$ recipient mice. The leukocyte distribution in lungs before the adoptive transfer (Upper panel) and at 48 h after adoptive transfer and LPS administration (lower panel) are presented. **B** Bar graphs representing the amount of WT and $\alpha 7nAChR$ -deficient macrophages detected in organs by flow cytometry. The experimental setup is same, as depicted in Fig. 3A, using 8-week-old male and female $\alpha 7nAChR^{-/-}$ recipients instead of WT ($n=4$). Statistical analysis was performed using a student’s *t* test. ** $P < 0.01$

$\alpha 7nAChR$ deficiency markedly reduces relative mRNA levels of integrins αM and αX

Based on the results obtained from our 3D migration assay and tracked adoptive transfer experiment, we hypothesized that the expression of chemokine receptors and adhesive receptors may be altered in $\alpha 7nAChR$ -deficient macrophages, leading to a decrease in their migration. We investigated the expression levels of

adhesion receptors from $\beta 2$ integrin family: αM , αD , αX and directly from $\beta 1$ integrin (which forms the complex with several α subunits, including $\alpha 2$, $\alpha 3$, $\alpha 4$, $\alpha 5$) as these receptors play a role in macrophage migration by interacting with extracellular matrix proteins. Chemokine receptors CCR2 and CCR5 were also examined, as they are major receptors in macrophage chemotaxis, as well as the respective receptors for MCP-1 and RANTES, the

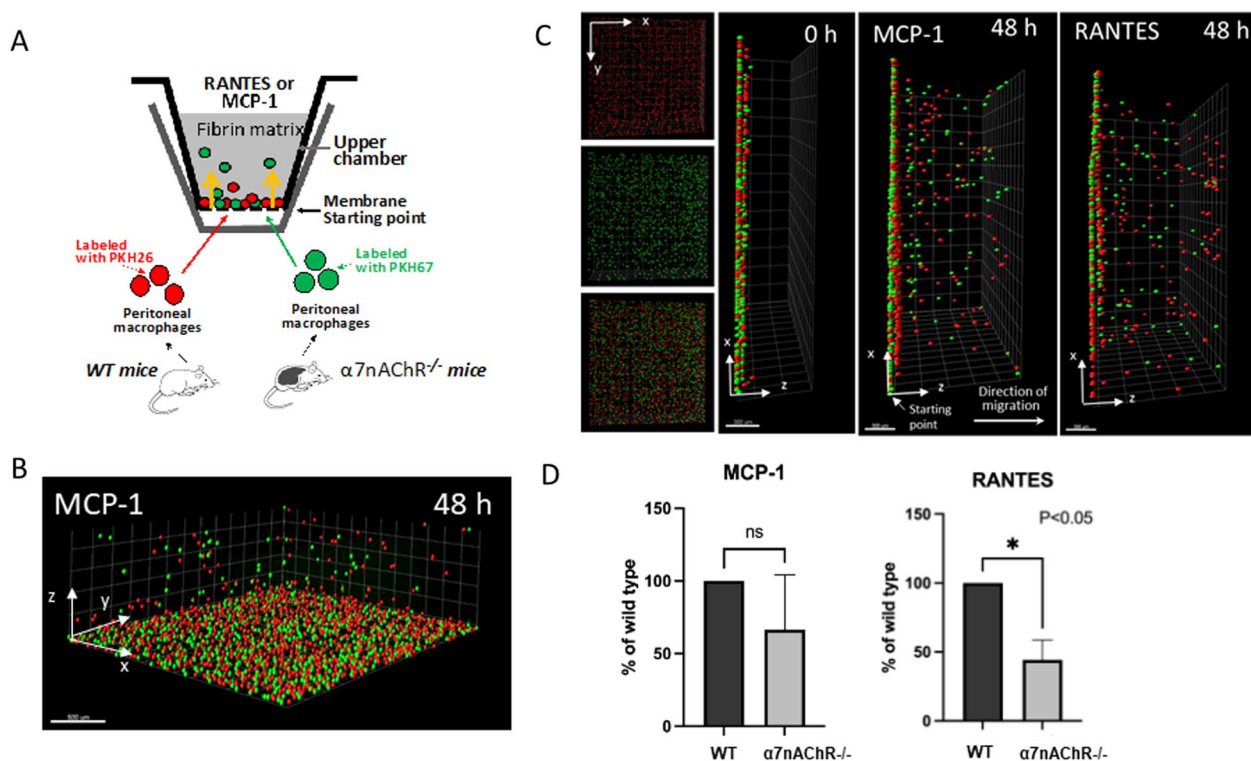


Fig. 5. 3-D migration of peritoneal macrophages along MCP-1 and RANTES gradients. **A** Schematic drawing of experimental setup within a Corning transwell insert, with yellow arrows indicating the direction of macrophage migration. WT macrophages were labeled red (PKH26) and $\alpha 7nAChR^{-/-}$ macrophages were labeled green (PKH67) before being added to the membrane. Migration was initiated using RANTES (12.8nM) or MCP-1 (30nM) in medium added to the top of the fibrin gel. **B** 3-D view of labeled macrophages migrating inside the fibrin gel after 48 h. **C** IMARIS 8.0 reconstruction of WT (red) and $\alpha 7nAChR^{-/-}$ (green) macrophages before the initiation of migration and after 48-h incubation. Left shows the top view of individual and combined channels. Center, side view showing starting point at 0h. Right, side view showing macrophages migrating along MCP-1 or RANTES gradients. **D** The number of macrophages migrating greater than 80 μ m was analyzed as a percentage of WT (MCP-1, $n=4$; RANTES, $n=3$). Statistical analysis was carried out using a student's t test. * $P < 0.05$

chemokines used in our 3-D migration assay. To assess the mRNA levels of these selected receptors, we performed quantitative real-time polymerase chain reaction (qRT-PCR) using thioglycolate-induced peritoneal macrophages that were incubated overnight with LPS (10ng/mL) and PNU-282987 (30 μ m). Total RNA was extracted from the macrophage lysate and used for qRT-PCR analysis. The specific primers used for detecting αM , αD , αX , CCR2, and CCR5 are listed in Table 1 of the methods section.

$\alpha 7nAChR$ -deficient macrophages exhibited similar relative mRNA levels of CCR2 and CCR5 compared to WT controls (Fig. 6A). However, the relative mRNA levels of integrins αM and αX in $\alpha 7nAChR$ -deficient macrophages showed a statistically significant decrease compared to WT controls (Fig. 6B). Integrin subunit $\beta 1$ did not show any significant changes in $\alpha 7nAChR$ deficient mice (Fig. 6B). Furthermore, we examined the relative mRNA levels of the corresponding chemokines, MCP-1 and RANTES, which are secreted by macrophages to attract

additional leukocytes to the site of inflammation. The transcription of RANTES and MCP-1 remained relatively unchanged by $\alpha 7nAChR$ deficiency (Fig. 6A).

These findings indicate that the deficiency of $\alpha 7nAChR$ leads to significant decreases in the relative mRNA levels of αM and αX in macrophages. These alterations in receptor expression may contribute to the impaired migration observed in $\alpha 7nAChR$ -deficient macrophages. In addition, the similar relative mRNA levels of CCR2, CCR5, RANTES, and MCP-1 rule out the possibility of an altered response in $\alpha 7nAChR$ deficient macrophages via these chemotactic mechanisms.

$\alpha 7nAChR$ deficiency reduces expression of αM at the cell surface of adoptively transferred monocytes

The macrophage expression of integrin αX is dramatically lower when compared with the level of integrin αM [42] (Additional file 1: Fig. S7). Due to its lower expression, αX is unlikely to significantly contribute to macrophage migration. Therefore, we focused primarily on

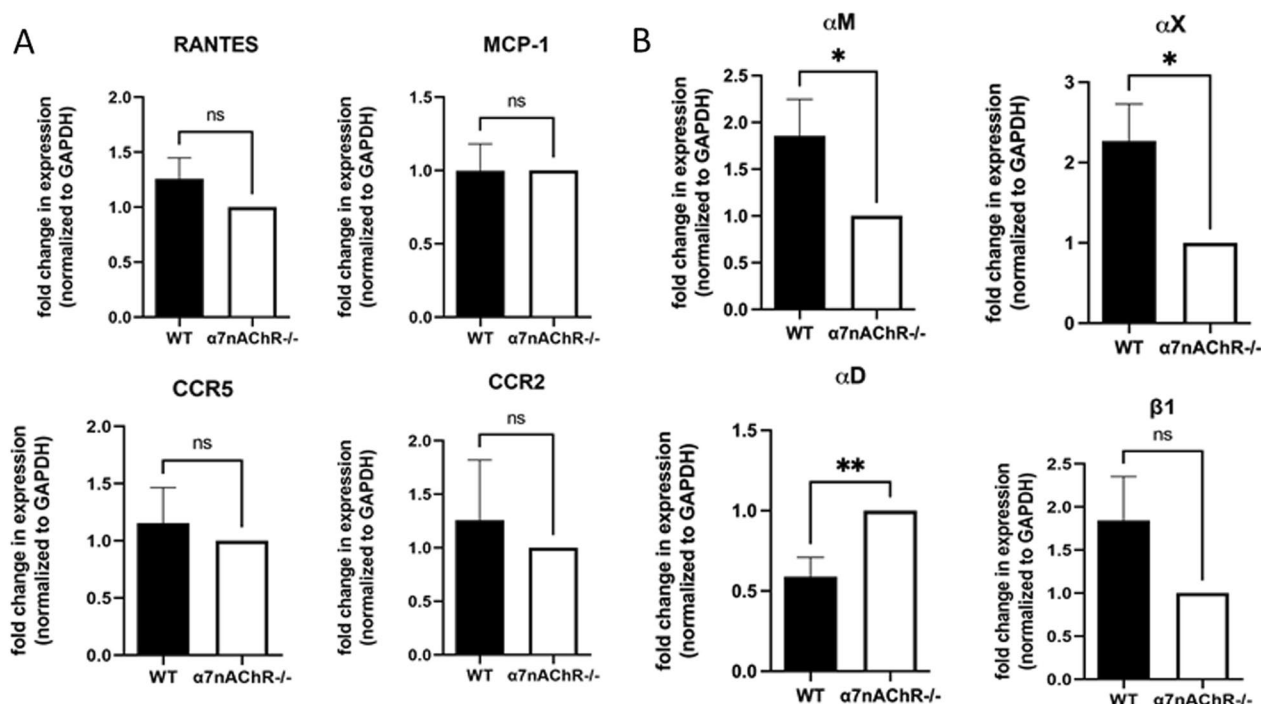


Fig. 6 Quantitative real-time PCR of chemokines and surface receptors. **A** Peritoneal macrophages were isolated from WT and $\alpha 7nAChR^{-/-}$ mice and subsequently incubated with LPS (10ng/mL) and PNU (30 μ M) overnight before isolation of RNA and production of cDNA. Plots show relative mRNA levels of CCR2 and its ligand MCP-1, and CCR5 and its ligand RANTES. **B** Cells were prepared for qRT-PCR identically to part A. Plots showing relative mRNA levels of integrin subunits αM , αX , αD , and $\beta 1$. Experiment had eight independent replicates. Data were analyzed using the Livak Method. Statistical analysis was performed with a student's *t* test. **P* < 0.05, ***P* < 0.01

αM . To verify our qPCR results, we assessed the expression levels of αM on adoptively transferred fluorescently labeled WT (PKH26) and $\alpha 7nAChR^{-/-}$ (PKH67) macrophages in lungs at 48 h after intraperitoneal injection of LPS (Fig. 7A–C). The expression of αM on adoptively transferred $\alpha 7nAChR$ -deficient (green) monocytes was significantly reduced compared to WT (red) monocytes (Fig. 7C). This finding suggests that $\alpha 7nAChR$ deficiency may affect the mesenchymal mode of macrophage migration, as αM plays a crucial role in the movement and adhesion of macrophages in the extracellular matrix.

Adoptive transfer of WT macrophages to $\alpha 7nAChR$ -deficient recipients leads to the partial rescue of phenotype

Since $\alpha 7nAChR$ expression on macrophages has a protective effect during endotoxemia, we reasoned that injecting WT monocytes into $\alpha 7nAChR$ -deficient mice could potentially rescue the protective phenotype of $\alpha 7nAChR$ and improve survival. Conversely, we also investigated whether injecting $\alpha 7nAChR$ -deficient monocytes to WT recipients would adversely affect survival.

First, we evaluated the potential effect of $\alpha 7nAChR$ -deficient monocytes injected to WT recipient mice.

WT mice were divided into two groups (n = 6/group) and injected with WT or $\alpha 7nAChR^{-/-}$ monocytes intravenously 5 min prior the induction of endotoxemia. In addition, a third group was injected with the same concentration of LPS without adoptively transferred monocytes. A schematic diagram illustrating the experimental setup is shown in Fig. 8A. Body temperature and morbidity of the mice were monitored twice daily for 4 days. We did not find significant differences in survival between the three groups (Fig. 8B).

To test a potential protective mechanism of WT monocytes, we divided $\alpha 7nAChR^{-/-}$ recipient mice into two groups (n = 12/group) and administered unlabeled WT or $\alpha 7nAChR^{-/-}$ monocytes intravenously prior to inducing endotoxemia. The mice were monitored for 4 days for changes in body temperature and morbidity (Fig. 8C). All $\alpha 7nAChR$ -deficient recipient mice injected with $\alpha 7nAChR^{-/-}$ monocytes died within 60 h, while the same strain injected with the WT monocytes demonstrated a modest improvement in survival (25%) (Fig. 8C). These results demonstrate a partially protective effect of WT monocyte transfer to $\alpha 7nAChR$ -deficient recipients.

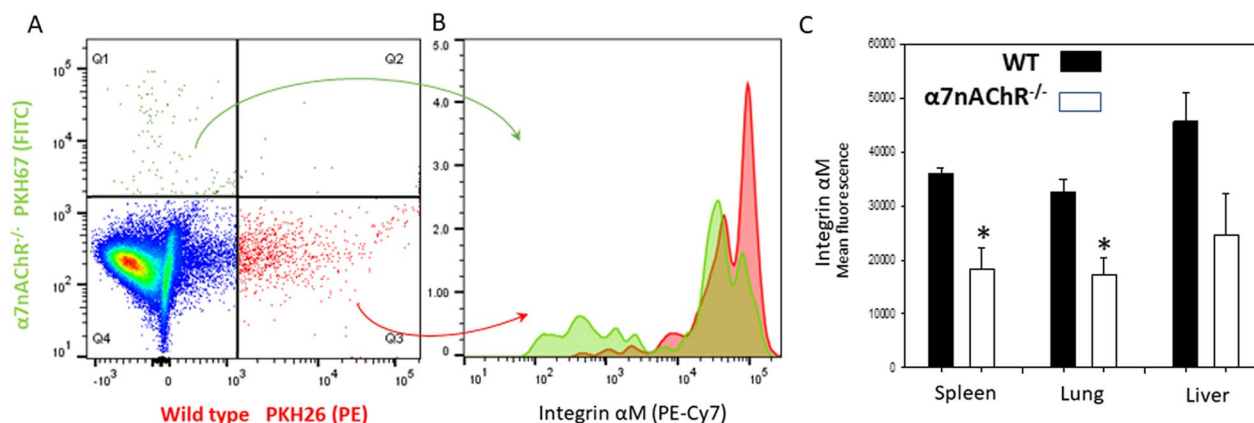


Fig. 7 Surface expression of integrin α M on migrating WT (red) and α 7nAChR^{-/-} (green) macrophages. **A** Representative flow cytometry dot plot showing migrated WT (red) and α 7nAChR^{-/-} (green) macrophages, in quadrant 3 and quadrant 1, respectively. **B** Histogram overlay of α M fluorescence, colors correspond to cell staining in part A. Data were analyzed using FlowJo software. **C** Bar graphs representing the amount of WT and α 7nAChR-deficient macrophages detected in organs by flow cytometry. ($n=4$). Statistical analysis was performed using student's *t* test. * $P<0.05$

Discussion

Here we showed that genetic α 7nAChR deficiency is associated with reduced macrophage migration to the lungs during murine endotoxemia and specific pharmacological activation of this receptor results in increased macrophage migration. These observations indicate a previously unrecognized role for the α 7nAChR, a key peripheral component of the cholinergic anti-inflammatory pathway, in mediating macrophage migration during acute inflammation. In parallel, α 7nAChR deficiency results in increased mortality of mice during endotoxemia, which indicates a tonic protective function of the α 7nAChR in inflammation. These findings identify macrophage migration as an important mechanism contributing to the physiological cholinergic regulation of inflammation. Additional mechanistic insight substantiates this notion, revealing that the expression of integrin α M β 2 is reduced on α 7nAChR-deficient monocyte-derived macrophages, indicating its potential role in α 7nAChR-mediated macrophage migration.

Macrophages are essential players in innate immunity that may have a protective or pathological contribution to the development of inflammatory diseases [23]. Macrophage phenotype, tissue distribution, molecular environment, and disease stage define the outcomes of macrophage function. Inhibition of pro-inflammatory cytokine secretion by macrophages was the major anti-inflammatory function reported for α 7nAChR [10, 43, 44]. Pioneering work from Kevin Tracey's group revealed that α 7nAChR activation blocks the nuclear translocation of NF- κ B, a master transcription factor for multiple pro-inflammatory genes that generate inflammatory responses [6, 12, 45–47]. However, other potential

mechanisms may have a significant contribution to the α 7nAChR-mediated macrophage response.

Despite a well-characterized protective role of α 7nAChR in endotoxemia and CLP sepsis, the direct effect of α 7nAChR-deficiency on survival during endotoxemia was not investigated previously. Our results of α 7nAChR^{-/-} mice compared with WT clearly demonstrate the detrimental impact of α 7nAChR deficiency on survival during murine endotoxemia and complement previous observations that administration of the α 7nAChR agonists GTS-21 or choline improve the survival of mice during endotoxemia and CLP sepsis [18, 19]. The significant drop of body temperature at 24 h after LPS-injection is an important pathophysiological effect of endotoxemia. Consequently, body temperature analysis was implemented as a reliable verification of endotoxemia severity and progression in our *in vivo* experiments.

Previous studies reported that the accumulation of macrophages in the lungs during sepsis can have a protective function [21, 22]. In contrast, the accumulation of neutrophils is a characteristic feature of sepsis-induced acute lung injury and is associated with poor outcomes [37, 48]. One of the mechanisms by which macrophages provide protection is through the control of inflammation via efferocytosis of activated neutrophils (Bailey et al. 2021). Here, we evaluated the effect of α 7nAChR activation using a specific agonist on macrophage accumulation in lungs. Previous studies demonstrated the potent anti-inflammatory effects of α 7nAChR activation by agonists, such as GTS-21 and PNU-282987 in murine models of systemic inflammation and sepsis [18, 19, 38, 44, 49]. We observed that wild-type mice treated with the agonist PNU-282987 exhibited a significant increase

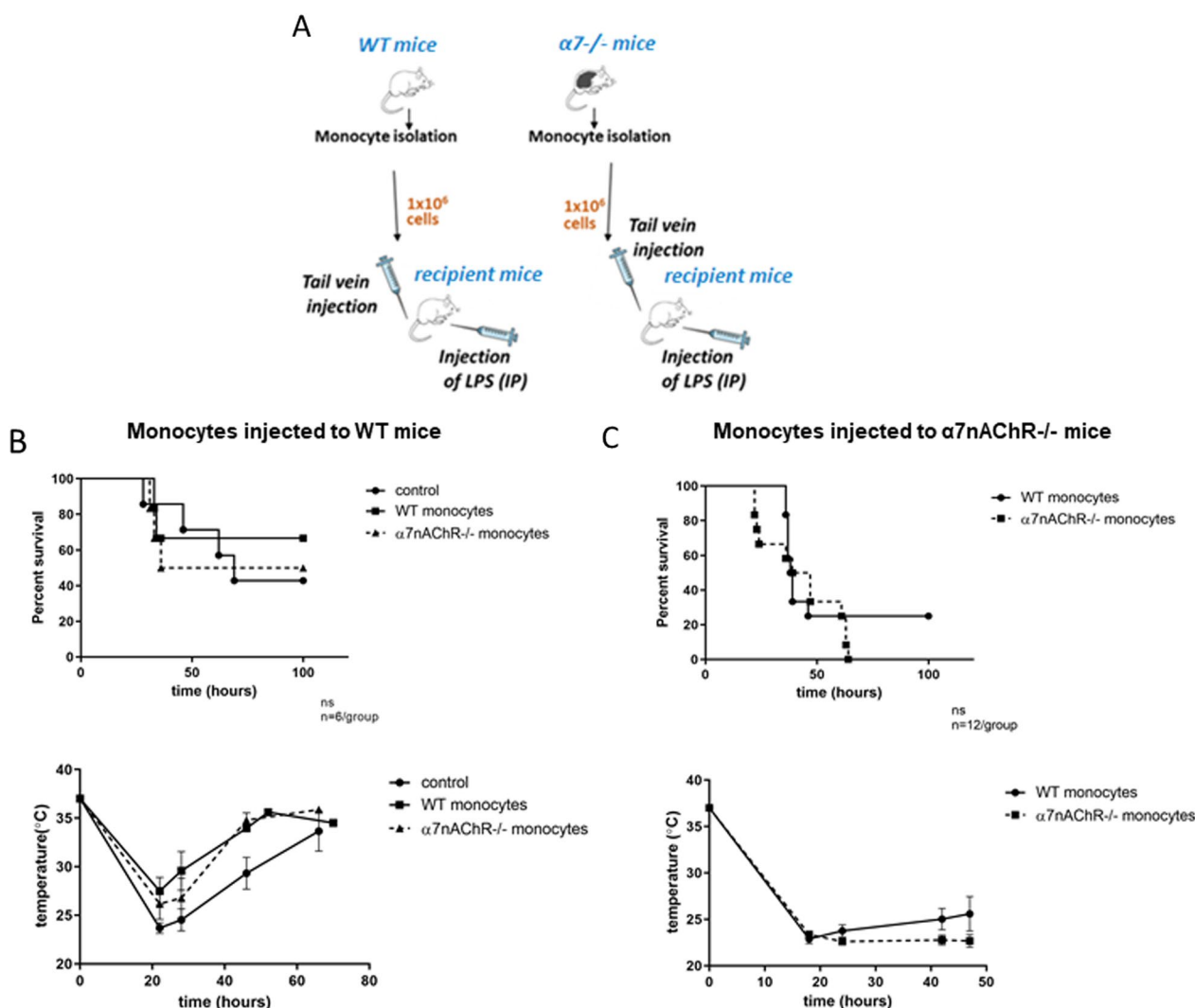


Fig. 8 Survival of WT and α7nAChR^{-/-} mice injected with monocytes during LPS-induced endotoxemia. **A** Graphical representation of experimental setup. Recipient mice are either WT (part B) or α7nAChR^{-/-} (part C). Control mice were given LPS only, with no monocytes. **B** Survival curve and temperature graph of WT recipients receiving WT, α7nAChR^{-/-}, or no monocytes (control) intravenously before a sub-lethal intraperitoneal dose of LPS. 8–10-week-old WT male and female mice were used as recipients (n=6/treatment group). **C** Survival curve and temperature graph of α7nAChR^{-/-} recipients receiving either WT or α7nAChR^{-/-} monocytes intravenously before a sub-lethal intraperitoneal dose of LPS. 8–10-week-old α7nAChR^{-/-} male and female mice were used as recipients (n=9/treatment group). For survival curves, statistical significance was assessed by the Kaplan–Meier method. Temperature graphs report mean temperature and standard error.

in the number of monocyte-derived macrophages and body temperature, along with a decrease in neutrophil numbers when compared to untreated mice. This finding is consistent with data reported by Huston et al. where nicotine treatment decreased the number of neutrophils accumulated in carrageenan-filled air pouches, as compared to controls [50].

Consistent with our α7nAChR activation approach, we observed a significant reduction in the number of macrophages in the lungs of α7nAChR-deficient mice during endotoxemia. These data were supported by the decrease

in body temperature in α7nAChR-deficient mice which indicates the greater severity of systemic inflammation in these animals.

To provide additional insights in our study, we evaluated *in vivo* migration by monitoring fluorescently labeled, adoptively transferred monocytes/macrophages in the model of endotoxemia [32, 40, 41, 51]. We employed an internal control within each recipient mouse by injecting an equal number of monocytes from both WT and α7nAChR^{-/-} donors, facilitating direct comparison between the two monocyte types. An

additional adoptive transfer tracking experiment was performed using $\alpha 7$ nAChR-deficient recipients. Both experiments revealed the same pattern: more WT monocytes were detected in the lungs, liver, and spleen when compared to $\alpha 7$ nAChR-deficient monocytes. In addition, to confirming the outcome of the experiment with WT recipients, the repetition with $\alpha 7$ nAChR-deficient recipients suggests that the enhanced migration of WT monocytes does not depend on the expression of $\alpha 7$ nAChR on other cell types. In both setups, the quality of the isolated donor monocytes was validated using flow cytometry, where a purity of 87–92% was confirmed.

To address any potential influence of fluorescent dyes on macrophage migration in vivo, we conducted a separate experiment comparing the migration of equal numbers of WT monocytes labeled with either PKH26 (red) or PKH67 (green) and found that both red and green-labeled WT macrophages exhibited similar motility when migrating towards inflamed tissue. These results provided evidence that the fluorescent dyes themselves do not significantly affect macrophage migration.

To demonstrate the direct involvement of $\alpha 7$ nAChR in macrophage migration, we conducted in vitro 3D migration assays, a well-developed technique that we have previously used [32, 40, 41]. Namely, our experimental setup provided a comprehensive assessment of macrophage migration, wherein monocyte-derived WT and $\alpha 7$ nAChR^{-/-} macrophages, labeled with different fluorescent dyes, migrated through a fibrin matrix against gravity in the presence of a chemokine gradient. By including two types of fluorescently labeled cells (WT and $\alpha 7$ nAChR^{-/-}) within the same matrix, we reduced data variability and enabled accurate calculation of the migration ratio between control and knockout macrophages in each sample. Within the fibrin matrix, we observed that $\alpha 7$ nAChR-deficient macrophages exhibited reduced effectiveness in migrating along both RANTES and MCP-1 gradients compared to WT macrophages.

In comparison with our experimental protocol, previous studies that attempted to evaluate the contribution of $\alpha 7$ nAChR to macrophage migration utilized macrophage-like cell lines, wild-type cell phenotype (no $\alpha 7$ nAChR-knockout), and the most importantly, a simplified 2D transmigration setup without chemokine gradients or protein coatings. For example, the ability of the $\alpha 7$ nAChR agonists (PHA-543613 and varenicline) to decrease migration of RAW264.7 cells was demonstrated by testing cell transmigration through uncoated trans-well membranes (Boyden chambers) without a chemokine gradient [52, 53]. Similar results were obtained by others who showed that acetylcholine can inhibit LPS-induced RAW264.7 cell migration. This study suggested that the inhibition of migration was attributed

to the blocking of MMP-9 expression [54]. MMPs play a role in 3D macrophage migration through the extracellular matrix (ECM) by degrading ECM proteins and creating space for cell movement. However, it should be noted that the presented experiments do not directly verify this hypothesis, as the proposed model using uncoated transwells does not involve MMP-mediated ECM degradation. In this model, macrophages transmigrate via an 8- μ m pore-size membrane without immobilized ligands and chemokine gradients, where cell motility is mostly regulated by gravity and diffusion. Therefore, the evaluation of the role of $\alpha 7$ nAChR in macrophage migration remained incomplete. In this study, we provided advanced characterization by implementing an improved experimental design and methodology.

In addition to migration through the extracellular matrix, trans-endothelial migration is another crucial step in the recruitment of leukocytes during inflammation. Our findings revealed no significant difference in the transmigration of WT and $\alpha 7$ nAChR^{-/-} monocytes across an endothelial monolayer in response to either MCP-1 or RANTES. These data were supported by the similar expression of integrins α L, α M, α 4, and L-selectin on WT and $\alpha 7$ nAChR^{-/-} mouse peripheral blood monocytes. These molecules are key adhesion receptors in the process of adhering to, and migrating across, the endothelial wall. Based on these results, we concluded that trans-endothelial migration does not contribute to the differential migration observed between WT and $\alpha 7$ nAChR^{-/-} monocytes/macrophages.

Reduced expression of integrin α X and integrin α M at the transcriptional level in $\alpha 7$ nAChR^{-/-} macrophages provides a potential mechanistic explanation for their reduced migration. Integrin α M β 2 is a crucial adhesive receptor for the recruitment of monocytes and migration of macrophages through the extracellular matrix. Integrin α X β 2 possesses multiple regulatory functions on macrophages [55, 56], but has a limited effect on macrophage migration due to relatively low level of expression on macrophage subsets. Therefore, the decreased α M mRNA and protein levels in $\alpha 7$ nAChR^{-/-} macrophages suggest that their impaired migration may be due to altered adhesion.

In contrast to these findings, we observed an increased expression of integrin α D β 2 in $\alpha 7$ nAChR^{-/-} macrophages. Integrin α D β 2 is significantly upregulated on pro-inflammatory (M1-like) macrophages in vivo and in vitro and contributes to the development of various chronic inflammatory diseases, such as atherosclerosis and diabetes [32, 41]. Importantly, previous studies have shown that activation of $\alpha 7$ nAChR leads to macrophage polarization toward the M2 phenotype [38, 39, 57]; therefore, $\alpha 7$ nAChR deficiency should be associated with M1

phenotype, where integrin $\alpha\text{D}\beta\text{2}$ is upregulated. Based on the levels of $\alpha\text{M}\beta\text{2}$ and $\alpha\text{D}\beta\text{2}$ expression on different macrophage subsets, it was suggested that $\alpha\text{M}\beta\text{2}$ is involved in macrophage migration to and from the sites of inflammation, while $\alpha\text{D}\beta\text{2}$ plays a role in the retention of pro-inflammatory, M1-polarized macrophages at the sites of chronic inflammation [40]. Therefore, the modest upregulation of the low-expressed $\alpha\text{D}\beta\text{2}$ on monocyte-derived macrophages may have a limited impact on macrophage migration but highlights the potential pathological role of integrin $\alpha\text{D}\beta\text{2}$ in α7nAChR -deficient mice during the development of atherosclerosis and diabetes [58–60].

Interestingly, the injection of WT monocytes did not completely rescue the phenotype of α7nAChR -deficient mice, resulting in only partial improvement in survival. It could be that this incomplete rescue is attributed to the already overwhelming NF- κB activation present in $\alpha\text{7nAChR}^{-/-}$ mice; thus, adding a population of WT monocytes may not be sufficient to reverse the deleterious effects caused by α7nAChR deficiency.

The recent discovery of *CHRFAM7A*, a human-specific dominant negative regulator of α7nAChR function expanded our understanding of how the cholinergic anti-inflammatory pathway is regulated in humans [61, 62]. The translated protein *CHRFAM7A* (*dup α7*) lacks the acetylcholine binding site, leading to reduced α7 receptor activity. In a study using peripheral blood mononuclear cells from septic patients, Cedillo et al. reported that *CHRFAM7A* has an inverse relationship with disease severity as well as cholinergic anti-inflammatory pathway activity, where patients with higher expression of *CHRFAM7A* had poorer prognoses [63]. THP-1 human monocytic cells transfected with *dup α7* demonstrated a reduced migration, colony formation, and chemotaxis toward MCP-1 [64]. Therefore, the reduced α7 receptor activity inhibits macrophage migration, aligning with our observation that α7nAChR deficiency has a negative impact on the migration of mouse macrophages. Despite the translational incongruency, basic research of α7nAChR and the cholinergic anti-inflammatory pathway thus far in rodents, primary human monocytes, and cell lines has provided invaluable insights and presented therapeutic opportunities for the treatment of sepsis.

Based on our results, we propose that α7nAChR deficiency leads to reduced migration of macrophages to the lungs and other inflamed organs, thereby impairing the clearance of recruited neutrophils through efferocytosis. Consequently, neutrophils present in the tissues of $\alpha\text{7nAChR}^{-/-}$ mice secrete pro-inflammatory cytokines. Furthermore, the failed recruitment of α7nAChR -deficient monocytes results in their

accumulation in the bloodstream and the secretion of pro-inflammatory cytokines via NF- κB -related mechanisms [65, 66]. Collectively, these processes contribute to an increased cytokine storm and higher mortality rate.

Conclusions

Our findings indicate that the cholinergic anti-inflammatory pathway, specifically the α7nAChR , plays a crucial role in regulating the migration and accumulation of macrophages at inflammation sites. We present evidence that α7nAChR is not only protective during endotoxemia but also essential for efficient monocyte/macrophage trafficking. Using α7nAChR -deficient mice or stimulating WT mice with PNU-282987, we demonstrate that the α7nAChR supports the recruitment of monocyte-derived macrophages to the lungs in vivo and their migration in a 3D matrix in vitro. α7nAChR deficiency adversely affects migration, which is associated with reduced levels of integrin $\alpha\text{M}\beta\text{2}$, a critical integrin involved in various stages of the leukocyte migration process. In summary, our findings provide novel insights into α7nAChR -mediated monocyte/macrophage migration to inflamed tissues, expanding the clinical possibilities for septic patients.

Abbreviations

α7nAChR	Alpha 7 nicotinic acetylcholine receptor
VNS	Vagal nerve stimulation
CLP	Cecal ligation and puncture
WT	Wild type
LPS	Lipopolysaccharide
ECM	Extracellular matrix

Supplementary Information

The online version contains supplementary material available at <https://doi.org/10.1186/s12974-023-03001-7>.

Additional file 1. Supplementary figures.

Acknowledgements

Not applicable.

Author contributions

KRK, VPY, KC, JLC, and SS performed experiments and collected resulting data. VPY, VAP, DVH, and DLW provided insight and supervision throughout the course of the project. All authors read and approved the final manuscript.

Funding

These studies were supported by the National Institutes of Health grants R15HL157836 (VPY), R01GM119197 and R01GM083016 (D.L.W.), R01GM128008 (VAP), and by the National Institute of Health grant C06RR0306551 for East Tennessee State University.

Availability of data and materials

The data sets used and/or analyzed during the current study are available from the corresponding author on reasonable request.

Declarations

Ethics approval and consent to participate

All animal procedures were performed according to animal protocols approved by East Tennessee State University IACUC.

Consent for publication

Not applicable.

Competing interests

The authors declare they have no competing interests.

Author details

¹Department of Biomedical Sciences, Quillen College of Medicine, East Tennessee State University, PO Box 70582, Johnson, TN, USA. ²Department of Surgery, Quillen College of Medicine, East Tennessee State University, Johnson, TN, USA. ³Center of Excellence in Inflammation, Infectious Disease and Immunity, East Tennessee State University, Johnson, TN, USA. ⁴Center for Biomedical Science and Center for Bioelectronic Medicine, The Feinstein Institute for Medical Research, Northwell Health, Manhasset, NY, USA. ⁵Donald and Barbara Zucker School of Medicine at Hofstra/Northwell, Hempstead, NY 11550, USA.

Received: 19 October 2023 Accepted: 19 December 2023

Published online: 04 January 2024

References

- Pavlov VA, Chavan SS, Tracey KJ. Molecular and functional neuroscience in immunity. *Annu Rev Immunol*. 2018;36:783–812.
- Tracey KJ. The inflammatory reflex. *Nature*. 2002;420(6917):853–9.
- Chavan SS, Pavlov VA, Tracey KJ. Mechanisms and therapeutic relevance of neuro-immune communication. *Immunity*. 2017;46(6):927–42.
- Pavlov VA, Tracey KJ. The vagus nerve and the inflammatory reflex—linking immunity and metabolism. *Nat Rev Endocrinol*. 2012;8(12):743–54.
- Pavlov VA, Wang H, Czura CJ, Friedman SG, Tracey KJ. The cholinergic anti-inflammatory pathway: a missing link in neuroimmunomodulation. *Mol Med*. 2003;9(5–8):125–34.
- Wang H, Yu M, Ochani M, Amella CA, Tanovic M, Susarla S, et al. Nicotinic acetylcholine receptor alpha7 subunit is an essential regulator of inflammation. *Nature*. 2003. <https://doi.org/10.1038/nature01339>.
- Keever KR, Yakubenko VP, Hoover DB. Neuroimmune nexus in the pathophysiology and therapy of inflammatory disorders: role of alpha7 nicotinic acetylcholine receptors. *Pharmacol Res*. 2023;191: 106758.
- Li Q, Zhou XD, Kolosov VP, Perelman JM. Nicotine reduces TNF- α expression through a alpha7 nAChR/MyD88/NF- κ B pathway in HBE16 airway epithelial cells. *Cell Physiol Biochem*. 2011;27(5):605–12.
- Parrish WR, Rosas-Ballina M, Gallowitsch-Puerta M, Ochani M, Ochani K, Yang LH, et al. Modulation of TNF release by choline requires alpha7 subunit nicotinic acetylcholine receptor-mediated signaling. *Mol Med*. 2008. <https://doi.org/10.2119/2008-00079.Parrish>.
- Rosas-Ballina M, Goldstein RS, Gallowitsch-Puerta M, Yang L, Valdes-Ferrer SI, Patel NB, et al. The selective alpha7 agonist GTS-21 attenuates cytokine production in human whole blood and human monocytes activated by ligands for TLR2, TLR3, TLR4, TLR9, and RAGE. *Mol Med*. 2009. <https://doi.org/10.2119/molmed.2009.00039>.
- Rosas-Ballina M, Ochani M, Parrish WR, Ochani K, Harris YT, Huston JM, et al. Splenic nerve is required for cholinergic antiinflammatory pathway control of TNF in endotoxemia. *Proc Natl Acad Sci U S A*. 2008. <https://doi.org/10.1073/pnas.0803237105>.
- Borovikova LV, Ivanova S, Zhang M, Yang H, Botchkina GI, Watkins LR, et al. Vagus nerve stimulation attenuates the systemic inflammatory response to endotoxin. *Nature*. 2000. <https://doi.org/10.1038/35013070>.
- Huston JM, Ochani M, Rosas-Ballina M, Liao H, Ochani K, Pavlov VA, et al. Splenectomy inactivates the cholinergic antiinflammatory pathway during lethal endotoxemia and polymicrobial sepsis. *J Exp Med*. 2006. <https://doi.org/10.1084/jem.20052362>.
- Pavlov VA, Tracey KJ. Bioelectronic medicine: preclinical insights and clinical advances. *Neuron*. 2022;110(21):3627–44.
- Buras JA, Holzmann B, Sitkovsky M. Animal models of sepsis: setting the stage. *Nat Rev Drug Discov*. 2005;4(10):854–65.
- Prescott HC, Angus DC. Enhancing recovery from sepsis: a review. *JAMA*. 2018. <https://doi.org/10.1001/jama.2017.17687>.
- Kim TH, Kim SJ, Lee SM. Stimulation of the alpha7 nicotinic acetylcholine receptor protects against sepsis by inhibiting Toll-like receptor via phosphoinositide 3-kinase activation. *J Infect Dis*. 2014. <https://doi.org/10.1093/infdis/jit669>.
- Nullens S, Staessens M, Peleman C, Schrijvers DM, Malhotra-Kumar S, Francque S, et al. Effect of GTS-21, an alpha7 nicotinic acetylcholine receptor agonist, on CLP-induced inflammatory, gastrointestinal motility, and colonic permeability changes in mice. *Shock*. 2016. <https://doi.org/10.1097/SHK.0000000000000519>.
- Pavlov VA, Ochani M, Yang LH, Gallowitsch-Puerta M, Ochani K, Lin X, et al. Selective alpha7-nicotinic acetylcholine receptor agonist GTS-21 improves survival in murine endotoxemia and severe sepsis. *Crit Care Med*. 2007. <https://doi.org/10.1097/01.CCM.0000259381.56526.96>.
- Huston JM, Gallowitsch-Puerta M, Ochani M, Ochani K, Yuan R, Rosas-Ballina M, et al. Transcutaneous vagus nerve stimulation reduces serum high mobility group box 1 levels and improves survival in murine sepsis. *Crit Care Med*. 2007. <https://doi.org/10.1097/01.CCM.0000288102.15975.BA>.
- Bailey WP, Cui K, Ardell CL, Keever KR, Singh S, Rodriguez-Gil DJ, et al. Frontline Science: The expression of integrin α D β 2 (CD11d/CD18) on neutrophils orchestrates the defense mechanism against endotoxemia and sepsis. *J Leukoc Biol*. 2021. <https://doi.org/10.1002/JLB.3HI0820-529RR>.
- Kumar V. Pulmonary innate immune response determines the outcome of inflammation during pneumonia and sepsis-associated acute lung injury. *Front Immunol*. 2020;11:1722.
- Parisi L, Gini E, Baci D, Tremolati M, Fanuli M, Bassani B, et al. Macrophage polarization in chronic inflammatory diseases: killers or builders? *J Immunol Res*. 2018;2018:8917804.
- Cai KC, van Mil S, Murray E, Mallet JF, Matar C, Ismail N. Age and sex differences in immune response following LPS treatment in mice. *Brain Behav Immun*. 2016;58:327–37.
- Kuo SM. Gender difference in bacteria endotoxin-induced inflammatory and anorexic responses. *PLoS ONE*. 2016;11(9): e0162971.
- Bailey WP, Cui K, Ardell CL, Keever KR, Singh S, Rodriguez-Gil DJ, Ozment TR, Williams DL, Yakubenko VP. The expression of integrin α D β 2 (CD11d/CD18) on neutrophils orchestrates the defense mechanism against endotoxemia and sepsis. *J Leukoc Biol*. 2021. <https://doi.org/10.1002/JLB.3HI0820-529RR>.
- Kawaguchi-Niida M, Yamamoto T, Kato Y, Inose Y, Shibata N. MCP-1/CCR2 signaling-mediated astrocytosis is accelerated in a transgenic mouse model of SOD1-mutated familial ALS. *Acta Neuropathol Commun*. 2013;1:21.
- Martín-Leal A, Blanco R, Casas J, Sáez ME, Rodríguez-Bovolenta E, de Rojas I, et al. CCR5 deficiency impairs CD4(+) T-cell memory responses and antigenic sensitivity through increased ceramide synthesis. *Embo J*. 2020;39(15): e104749.
- Livak KJ, Schmittgen TD. Analysis of relative gene expression data using real-time quantitative PCR and the 2(-Delta Delta C(T)) Method. *Methods*. 2001;25(4):402–8.
- Favaretto F, Milan G, Collin GB, Marshall JD, Stasi F, Maffei P, et al. GLUT4 defects in adipose tissue are early signs of metabolic alterations in Alms1GT/GT, a mouse model for obesity and insulin resistance. *PLoS ONE*. 2014;9(10): e109540.
- Zhang F, Li Y, Tang Z, Kumar A, Lee C, Zhang L, et al. Proliferative and survival effects of PUMA promote angiogenesis. *Cell Rep*. 2012;2(5):1272–85.
- Aziz MH, Cui K, Das M, Brown KE, Ardell CL, Febbraio M, et al. The upregulation of integrin α (D) β (2) (CD11d/CD18) on inflammatory macrophages promotes macrophage retention in vascular lesions and development of atherosclerosis. *J Immunol*. 2017;198(12):4855–67.
- Patsouris D, Cao JJ, Vial G, Bravard A, Lefai E, Durand A, et al. Insulin resistance is associated with MCP1-mediated macrophage accumulation in skeletal muscle in mice and humans. *PLoS ONE*. 2014;9(10): e110653.
- Perrin J, Capitaio M, Allard M, Chouin N, Gouard S, Marionneau-Lambot S, et al. Targeted alpha particle therapy remodels the tumor microenvironment and improves efficacy of immunotherapy. *Int J Radiat Oncol Biol Phys*. 2022;112(3):790–801.

35. Sutherland AE, Calarco PG, Damsky CH. Developmental regulation of integrin expression at the time of implantation in the mouse embryo. *Development*. 1993;119(4):1175–86.
36. Kuefner MS, Pham K, Redd JR, Stephenson EJ, Harvey I, Deng X, et al. Secretory phospholipase A(2) group IIA modulates insulin sensitivity and metabolism. *J Lipid Res*. 2017;58(9):1822–33.
37. Grommes J, Soehnlein O. Contribution of neutrophils to acute lung injury. *Mol Med*. 2011. <https://doi.org/10.2119/molmed.2010.00138>.
38. Pinheiro NM, Santana FP, Almeida RR, Guerreiro M, Martins MA, Caperuto LC, et al. Acute lung injury is reduced by the alpha7nAChR agonist PNU-282987 through changes in the macrophage profile. *FASEB J*. 2017. <https://doi.org/10.1096/fj.201600431R>.
39. Wang J, Li R, Peng Z, Zhou W, Hu B, Rao X, et al. GTS-21 reduces inflammation in acute lung injury by regulating m1 polarization and function of alveolar macrophages. *Shock*. 2019. <https://doi.org/10.1097/SHK.0000000000001144>.
40. Cui K, Ardell CL, Podolnikova NP, Yakubenko VP. Distinct migratory properties of M1, M2, and resident macrophages are regulated by alpha(D) beta(2) and alpha(M)beta(2) integrin-mediated adhesion. *Front Immunol*. 2018;9:2650.
41. Cui K, Podolnikova NP, Bailey W, Szmuc E, Podrez EA, Byzova TV, et al. Inhibition of integrin alpha(D)beta(2)-mediated macrophage adhesion to end product of docosahexaenoic acid (DHA) oxidation prevents macrophage accumulation during inflammation. *J Biol Chem*. 2019;294(39):14370–82.
42. Tang Z, Davidson D, Li R, Zhong MC, Qian J, Chen J, et al. Inflammatory macrophages exploit unconventional pro-phagocytic integrins for phagocytosis and anti-tumor immunity. *Cell Rep*. 2021;37(11): 110111.
43. Ulleryd MA, Mjornstedt F, Panagaki D, Yang LJ, Engevall K, Gutierrez S, et al. Stimulation of alpha 7 nicotinic acetylcholine receptor (alpha-7nAChR) inhibits atherosclerosis via immunomodulatory effects on myeloid cells. *Atherosclerosis*. 2019. <https://doi.org/10.1016/j.atherosclerosis.2019.06.903>.
44. Yue Y, Liu R, Cheng W, Hu Y, Li J, Pan X, et al. GTS-21 attenuates lipopolysaccharide-induced inflammatory cytokine production in vitro by modulating the Akt and NF-kappaB signaling pathway through the alpha7 nicotinic acetylcholine receptor. *Int Immunopharmacol*. 2015;29(2):504–12.
45. Pavlov VA, Tracey KJ. The cholinergic anti-inflammatory pathway. *Brain Behav Immun*. 2005;19(6):493–9.
46. Tracey KJ. Reflex control of immunity. *Nat Rev Immunol*. 2009;9(6):418–28.
47. Wang H, Liao H, Ochani M, Justiniani M, Lin X, Yang L, et al. Cholinergic agonists inhibit HMGB1 release and improve survival in experimental sepsis. *Nat Med*. 2004. <https://doi.org/10.1038/nm1124>.
48. Sessler CN, Bloomfield GL, Fowler AA 3rd. Current concepts of sepsis and acute lung injury. *Clin Chest Med*. 1996;17(2):213–35.
49. Shi X, Li J, Han Y, Wang J, Li Q, Zheng Y, et al. The alpha7nAChR agonist PNU-282987 ameliorates sepsis-induced acute kidney injury via CD4+CD25+ regulatory T cells in rats. *Bosn J Basic Med Sci*. 2022. <https://doi.org/10.17305/bjbm.2022.7111>.
50. Huston JM, Rosas-Ballina M, Xue X, Dowling O, Ochani K, Ochani M, et al. Cholinergic neural signals to the spleen down-regulate leukocyte trafficking via CD11b. *J Immunol*. 2009;183(1):552–9.
51. Cao C, Lawrence DA, Strickland DK, Zhang L. A specific role of integrin Mac-1 in accelerated macrophage efflux to the lymphatics. *Blood*. 2005;106(9):3234–41.
52. Baris E, Efe H, Gumustekin M, Arici MA, Tosun M. Varenicline prevents LPS-induced inflammatory response via nicotinic acetylcholine receptors in RAW 264.7 macrophages. *Front Mol Biosci*. 2021. <https://doi.org/10.3389/fmols.2021.721533>.
53. Liu EYL, Xia Y, Kong X, Guo MSS, Yu AXD, Zheng BZY, et al. Interacting with alpha7 nAChR is a new mechanism for AChE to enhance the inflammatory response in macrophages. *Acta Pharm Sin B*. 2020. <https://doi.org/10.1016/j.apsb.2020.05.005>.
54. Yang YH, Li DL, Bi XY, Sun L, Yu XJ, Fang HL, et al. Acetylcholine inhibits LPS-induced MMP-9 production and cell migration via the alpha7 nAChR-JAK2/STAT3 pathway in RAW2647 cells. *Cell Physiol Biochem*. 2015;36(5):2025–38.
55. Wu H, Gower RM, Wang H, Perrard XY, Ma R, Bullard DC, et al. Functional role of CD11c+ monocytes in atherogenesis associated with hypercholesterolemia. *Circulation*. 2009;119(20):2708–17.
56. Wang Q, Su X, He Y, Wang M, Yang D, Zhang R, et al. CD11c participates in triggering acute graft-versus-host disease during bone marrow transplantation. *Immunology*. 2021;164(1):148–60.
57. Zhang Q, Lu Y, Bian H, Guo L, Zhu H. Activation of the alpha7 nicotinic receptor promotes lipopolysaccharide-induced conversion of M1 microglia to M2. *Am J Transl Res*. 2017;9:971–85.
58. Johansson ME, Ulleryd MA, Bernardi A, Lundberg AM, Andersson A, Folkersen L, et al. Alpha7 Nicotinic acetylcholine receptor is expressed in human atherosclerosis and inhibits disease in mice—brief report. *Arterioscler Thromb Vasc Biol*. 2014. <https://doi.org/10.1161/ATVBAHA.114.303892>.
59. Gausseres B, Liu J, Foppen E, Tourrel-Cuzin C, Rodriguez Sanchez-Archidona A, Delangre E, et al. The constitutive lack of alpha7 nicotinic receptor leads to metabolic disorders in mouse. *Biomolecules*. 2020. <https://doi.org/10.3390/biom10071057>.
60. Wilund KR, Rosenblat M, Chung HR, Volkova N, Kaplan M, Woods JA, et al. Macrophages from alpha 7 nicotinic acetylcholine receptor knockout mice demonstrate increased cholesterol accumulation and decreased cellular paraoxonase expression: a possible link between the nervous system and atherosclerosis development. *Biochem Biophys Res Commun*. 2009. <https://doi.org/10.1016/j.bbrc.2009.09.088>.
61. Di Lascio S, Fornasari D, Benfante R. The human-restricted isoform of the alpha7 nAChR, CHRFA7A: a double-edged sword in neurological and inflammatory disorders. *Int J Mol Sci*. 2022. <https://doi.org/10.3390/ijms23073463>.
62. Peng W, Mao L, Dang X. The emergence of the uniquely human alpha7 nicotinic acetylcholine receptor gene and its roles in inflammation. *Gene*. 2022. <https://doi.org/10.1016/j.gene.2022.146777>.
63. Cedillo JL, Arnalich F, Martín-Sánchez C, Quesada A, Rios JJ, Maldifassi MC, et al. Usefulness of alpha7 nicotinic receptor messenger RNA levels in peripheral blood mononuclear cells as a marker for cholinergic anti-inflammatory pathway activity in septic patients: results of a pilot study. *J Infect Dis*. 2015;211(1):146–55.
64. Chan TW, Langness S, Cohen O, Eliceiri BP, Baird A, Costantini TW. CHRFA7A reduces monocyte/macrophage migration and colony formation in vitro. *Inflamm Res*. 2020. <https://doi.org/10.1007/s00011-020-01349-7>.
65. Schloss MJ, Hulsmans M, Rohde D, Lee IH, Severe N, Foy BH, et al. B lymphocyte-derived acetylcholine limits steady-state and emergency hematopoiesis. *Nat Immunol*. 2022. <https://doi.org/10.1038/s41590-022-01165-7>.
66. Saeed RW, Varma S, Peng-Nemeroff T, Sherry B, Balakhaneh D, Huston J, et al. Cholinergic stimulation blocks endothelial cell activation and leukocyte recruitment during inflammation. *J Exp Med*. 2005. <https://doi.org/10.1084/jem.20040463>.

Publisher's Note

Springer Nature remains neutral with regard to jurisdictional claims in published maps and institutional affiliations.

Ready to submit your research? Choose BMC and benefit from:

- fast, convenient online submission
- thorough peer review by experienced researchers in your field
- rapid publication on acceptance
- support for research data, including large and complex data types
- gold Open Access which fosters wider collaboration and increased citations
- maximum visibility for your research: over 100M website views per year

At BMC, research is always in progress.

Learn more biomedcentral.com/submissions

